

A combined diffraction and EXAFS study of LaCoO_3 and $\text{La}_{0.5}\text{Sr}_{0.5}\text{Co}_{0.75}\text{Nb}_{0.25}\text{O}_3$ powders

E. A. Efimova,^{1,(a)} V. V. Sikolenko,^{1,2} D. V. Karpinsky,³ I. O. Troyanchuk,³ S. Pascarelli,⁴ C. Ritter,⁵ M. Feyngenson,⁶ S. I. Tiutiunnikov,¹ and V. Efimov¹

¹Joint Institute for Nuclear Research, 141980 Dubna, Russia

²REC “Functional nanomaterials” Immanuel Kant Baltic Federal University, 236041 Kaliningrad, Russia

³Scientific-Practical Material Research Center NAS Belarus, 220072 Minsk, Belarus

⁴European Synchrotron Radiation Facility, BP 220, 38043 Grenoble, France

⁵Institut Laue-Langevin, Grenoble, France

⁶Jülich Centre for Neutron Science, Forschungszentrum Jülich GmbH, 52425 Jülich, Germany

(Received 13 September 2016; accepted 4 January 2017)

A combination of neutron diffraction, synchrotron X-ray diffraction, and high-resolution extended X-ray absorption fine structure measurements has been used to clarify the correlations between long- and local-range structural distortions across the spin-state transition in powders of LaCoO_3 and $\text{La}_{0.5}\text{Sr}_{0.5}\text{Co}_{0.75}\text{Nb}_{0.25}\text{O}_3$. The analysis of the diffraction data has revealed that the isotropic thermal parameters of Co–O bond abnormally increase below 100 K in both samples, while the temperature dependence of the average Co–O bond lengths is linear from 10 to 300 K. We also have found that the Co–O bond lengths are larger in $\text{La}_{0.5}\text{Sr}_{0.5}\text{Co}_{0.75}\text{Nb}_{0.25}\text{O}_3$, as compared with the ones in LaCoO_3 . The X-ray absorption data showed an anomalous decrease of the Co–O bond lengths only for LaCoO_3 , in contrast to the bond length values obtained by diffraction. The structural anomalies observed by spectroscopy measurements are discussed in terms of the spin-state transition model. © 2017 International Centre for Diffraction Data. [doi:10.1017/S0885715617000082]

Key words: neutron diffraction, EXAFS, Rietveld analyses, cobaltites

I. INTRODUCTION

$\text{La}_{1-x}\text{Sr}_x\text{CoO}_3$ ceramics attract much interest owing to the unusual structural, magnetic and transport properties, which are correlated with the spin-state configuration of the cobalt ion (Senaris-Rodriguez and Goodenough, 1995; Radaelli and Cheong, 2002; Zobel *et al.*, 2002; Maris *et al.*, 2003; Knížek *et al.*, 2005; Sazonov *et al.*, 2009). In the ground state, the parent compound LaCoO_3 contains the Co^{3+} ions in the low-spin electronic configuration $t_{2g}^6e_g^0$ (LS, $S=0$). The electronic configuration of Co^{3+} gradually changes to the intermediate (IS, $t_{2g}^5e_g^1$, $S=1$) or high (HS, $t_{2g}^4e_g^2$, $S=2$) spin state with temperature growth. The evolution of the electronic configuration of the cobalt ions can be probed experimentally owing to the significant difference in the ionic radii of the different spin states. In the HS, Co^{3+} has a considerably larger radius (0.61 Å) than in the LS (0.54 Å) and in the IS (0.55 Å) states (Shannon, 1976).

The redistribution of the electrons between the t_{2g} and e_g levels is a result of the competition between the crystal field splitting energy Δ_{cf} and the intra-atomic Hund exchange energy J_{ex} , which are comparable in cobaltites. The energy Δ_{cf} strongly depends on the Co–O bond length and therefore a balance between Δ_{cf} and J_{ex} can be easily adjusted by changing the temperature, external pressure or chemical substitution (Zobel *et al.*, 2002; Maris *et al.*, 2003; Knížek *et al.*, 2005).

The magnetic and transport properties of $\text{La}_{1-x}\text{Sr}_x\text{CoO}_3$ cobaltites with the perovskite-like structure are similar to those of the $\text{La}_{1-x}\text{Sr}_x\text{MnO}_3$ manganites (Maris *et al.*, 2003; Troyanchuk *et al.*, 2013a). In both systems, the substitution of La with divalent Sr ion induces a paramagnetic ($x < 0.15$) to ferromagnetic ($x > 0.3$) transition, as the dopant concentration increases. The ionic radius of Sr^{2+} is significantly larger than that of the La^{3+} ion, so it is possible to expect a stabilization of the IS state of the cobalt ions by substituting Sr^{2+} with La^{3+} ions. However, such heterovalent substitution results in the formation of Co^{4+} ions and leads consequently to the ferromagnetic metallic ground state (Knížek *et al.*, 2005). In order to prevent formation of the Co^{4+} ions, diamagnetic Nb ions can be introduced, which in the presence of Co^{3+} ions have the oxidation state of 5+. The simultaneous doping with both Sr^{2+} and Nb^{5+} ions preserves the oxidation state of the cobalt ions and therefore, the conductivity of $\text{La}_{1-x}\text{Sr}_x\text{Co}_{1-y}\text{Nb}_y\text{O}_3$ solid solutions would decrease with dopant concentration (Sikolenko *et al.*, 2009). Thus, the transition of the cobalt ions spin state from LS to the mixture of IS and HS, leads to modification of the exchange interaction $\text{Co}^{3+}\text{--O--Co}^{3+}$ (Potze *et al.*, 1995; Korotin *et al.*, 1996; Sundaram *et al.*, 2009).

In this work, we discuss the effects of temperature and doping on the structural and electronic properties of the cobalt ions in the LaCoO_3 and $\text{La}_{0.5}\text{Sr}_{0.5}\text{Co}_{0.75}\text{Nb}_{0.25}\text{O}_3$ compounds, based on neutron powder diffraction (NPD), X-ray powder diffraction (XRD), and extended X-ray absorption fine structure (EXAFS) measurements.

a) Author to whom correspondence should be addressed. Electronic mail: efea@mail.ru

II. EXPERIMENTAL

The synthesis of the powder samples of LaCoO_3 and $\text{La}_{0.5}\text{Sr}_{0.5}\text{Co}_{0.75}\text{Nb}_{0.25}\text{O}_3$ is described elsewhere (Sikolenko *et al.*, 2009). XRD experiments were carried out at the synchrotron facility HASYLAB/DESY (Hamburg, Germany) using the powder diffractometer at the B2 beamline in the temperature range of 17–300 K. The neutron diffraction experiments for the $\text{La}_{0.5}\text{Sr}_{0.5}\text{Co}_{0.75}\text{Nb}_{0.25}\text{O}_3$ sample were performed using the high-resolution powder diffractometer D2B at the Institute Laue-Langevin with the neutron wavelength of $\lambda = 1.594 \text{ \AA}$. The XRD and NPD data were analyzed by a Rietveld method using the FullProf program (Rodríguez-Carvajal, 1993).

EXAFS experiments have been performed at the beamline BM29 of the European Synchrotron Radiation Facility (ESRF) (Grenoble, France). The EXAFS spectra were measured at the Co *K*-edge in the energy range 7400–9500 eV in the standard transmission mode, simultaneously with a reference sample (9 μm cobalt) in the temperature range 20–300 K. Each temperature point was measured three times with a count rate of 2.5 s per point. To reduce the harmonic content in the X-ray beam, we detuned the monochromator crystals 40% at 7900 eV. The powder samples were deposited on the millipore cellulose membranes with thicknesses specially selected to obtain an X-ray absorption edge jump $\Delta\mu \cdot x \sim 1$ at the Co *K*-edge.

A curve-fitting procedure by the EDA software package (Kuzmin, 1995) was used to determine the average $R(\text{Co}-\text{O})$ distance and the parallel mean-square relative displacement (MSRD_{\parallel}) $\Delta\sigma_{\text{Co}-\text{O}}^2$ (or EXAFS Debye–Waller parameter). The energy position E_0 , used in the definition of the photoelectron wave number $k = [(2m_e/h^2)(E - E_0)]^{1/2}$, was set at the threshold energy $E_0 = 7714 \text{ eV}$. The Fourier transforms (FTs) of the EXAFS $\chi(k)k^2$ spectra were calculated in the wave number intervals up to $k = 1.0\text{--}20 \text{ \AA}^{-1}$ with a 10% Gaussian-type window function. At low temperatures up to 20 \AA^{-1} the signal-to-noise ratio is very good, however it deteriorates at high k as the temperature increases and it is rather poor beyond $\sim 18.0 \text{ \AA}^{-1}$ at 300 K. Consequently, in all the fits the upper end of the FT k range is restricted to 17.5 \AA^{-1} .

Experimental scattering amplitude and phase shift functions for the Co–O atom pair were used in the EXAFS analysis. They were obtained from the EXAFS spectra of a reference Co-foil sample at $T = 20 \text{ K}$. We assumed that under these conditions, anharmonicity effects in the dynamics of the CoO_6 octahedron can be neglected, and the sample was assumed to be composed of regular CoO_6 octahedra. The cobalt coordination number and Co–O distance were fixed to $N_{\text{ref}} = 6$ and $R_{\text{ref}} = 1.925 \text{ \AA}$, respectively, based on the Rietveld refinement of NPD data on the same LaCoO_3 sample.

III. RESULTS AND DISCUSSIONS

Figure 1 shows an example of the diffraction pattern for $\text{La}_{0.5}\text{Sr}_{0.5}\text{Co}_{0.75}\text{Nb}_{0.25}\text{O}_3$ at 5 K. All observed Bragg peaks for $\text{La}_{0.5}\text{Sr}_{0.5}\text{Co}_{0.75}\text{Nb}_{0.25}\text{O}_3$ and LaCoO_3 were indexed within the rhombohedral $R\bar{3}c$ space group and the structure does not change in the temperature range between 10 and 300 K.

Figure 2 shows the temperature dependence of the Co–O bond lengths for LaCoO_3 and $\text{La}_{0.5}\text{Sr}_{0.5}\text{Co}_{0.75}\text{Nb}_{0.25}\text{O}_3$ calculated using the refinement of the diffraction and the EXAFS

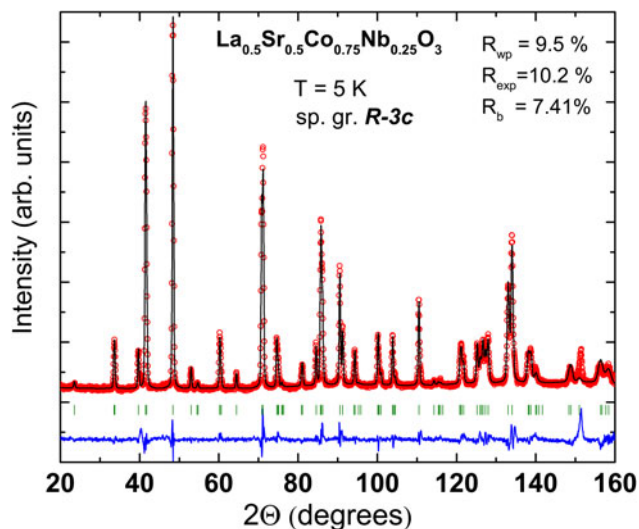


Figure 1. (Colour online) Rietveld refinement of NPD pattern collected for $\text{La}_{0.5}\text{Sr}_{0.5}\text{Co}_{0.75}\text{Nb}_{0.25}\text{O}_3$ at 5 K, with experimental data as open circles, the calculated pattern – black solid line, and the difference curve marked – blue line. The vertical ticks mark the corresponding positions of the Bragg reflections.

data. We note that the local interatomic distance $\langle r_{\text{Co}-\text{O}} \rangle = \langle |r_{\text{O}} - r_{\text{Co}}| \rangle$ (where r_{O} and r_{Co} are equilibrium interatomic distance between absorbing cobalt and backscattering oxygen atoms) probed by EXAFS is normally larger than the equilibrium crystallographic distance $R_{\text{Co}-\text{O}} = | \langle r_{\text{O}} \rangle - \langle r_{\text{Co}} \rangle |$ (where $\langle r_{\text{O}} \rangle$ and $\langle r_{\text{Co}} \rangle$ are average positions of oxygen and cobalt in unit cell) measured by diffraction techniques. For initial compound LaCoO_3 the Co–O bond lengths determined from the EXAFS analysis in our experiment are always shorter with respect to those obtained from the diffraction, and this deviation increases with temperature. Usually owing to perpendicular vibrations, the EXAFS bond lengths increase with temperature faster than that calculated from diffraction in framework of the same symmetry. Therefore the anomalous decrease of local atomic EXAFS Co–O bond lengths compared to long-range Co–O bond lengths calculated from the diffraction data above $\sim 80 \text{ K}$ could be explained by the gradually spin-state transition from LS (basic volume of 500 nm

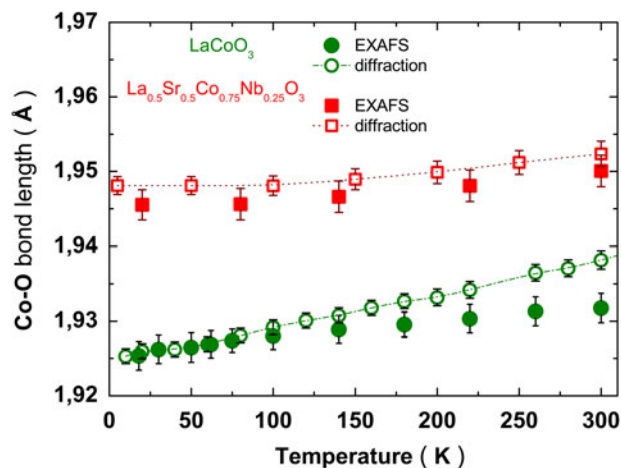


Figure 2. (Colour online) The temperature dependence of the Co–O bond lengths for LaCoO_3 and $\text{La}_{0.5}\text{Sr}_{0.5}\text{Co}_{0.75}\text{Nb}_{0.25}\text{O}_3$ obtained by EXAFS, NPD, and XRD.

powder grains) +HS (distorted surface layer of 500 nm powders) to LS +highly hybridized IS (from HS-distorted surface layer) that occurs at ~ 80 K and the IS/HS ratio is further increasing in LS with temperature. It is in agreement with similar radii of the LS (0.54 Å) and IS (0.56 Å) ions, compared with the HS ion radius (0.61 Å) (Shannon, 1976). In other words, the Co–O distance in the HS state is essentially longer than that of in the LS and IS states. As a consequence, an appearance of highly hybridized IS leads to a decrease of the perpendicular vibrations amplitude (compared with the HS ion and its longer radius), which is responsible for the increase of Co–O bond length.

It is interesting to note that the Co–O bond length obtained by EXAFS in the $\text{La}_{0.5}\text{Sr}_{0.5}\text{Co}_{0.75}\text{Nb}_{0.25}\text{O}_3$ sample is a little smaller up to room temperature than the ones obtained by diffraction. Presumably, it is associated with increased fraction of cobalt ions being in IS and especially HS states (which are mainly located in the surface layer of the grains), while a dominant amount of the cobalt ions retain the LS configuration in contrast to the situation occurred in LaCoO_3 at low temperatures (Figure 2).

The temperature dependencies of correlated MSRD_{\parallel} and of the uncorrelated mean-squared displacement (MSD or Debye–Waller parameter, calculated from diffraction data) for the Co–O bond in LaCoO_3 and $\text{La}_{0.5}\text{Sr}_{0.5}\text{Co}_{0.75}\text{Nb}_{0.25}\text{O}_3$ are shown in Figure 3. The MSD of Co–O bond exhibits an anomalous increase below ~ 50 K for both samples. This transition is more pronounced in the LaCoO_3 sample owing to considerably higher slope of the MSD at room temperature as compared to that attributed to the $\text{La}_{0.5}\text{Sr}_{0.5}\text{Co}_{0.75}\text{Nb}_{0.25}\text{O}_3$ sample.

The displacement correlation function (DCF) (i.e. difference between MSD and MSRD_{\parallel}), reflecting the correlation in atomic motion of distant cobalt and oxygen atoms increases gradually as a function of temperature (Figure 3) for both samples. Such increase of the interaction strength between atoms in the Co–O pairs can be associated with a gradual transition from HS Co^{3+} ions to a highly hybridized IS state (Korotin *et al.*, 1996; Pirogov *et al.*, 1999a; Sazonov *et al.*, 2009). In the $\text{La}_{0.5}\text{Sr}_{0.5}\text{Co}_{0.75}\text{Nb}_{0.25}\text{O}_3$ sample the DCF temperature

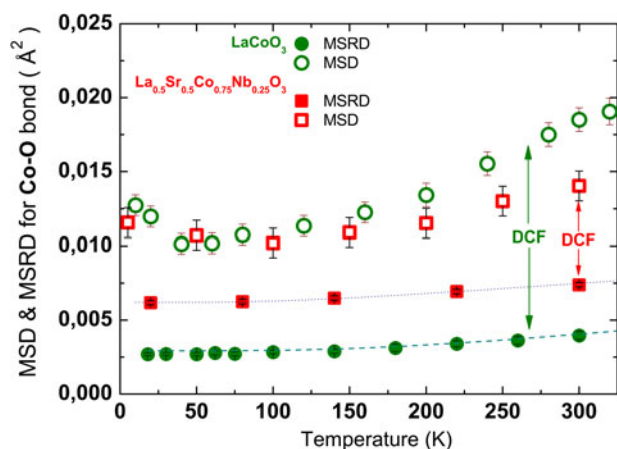


Figure 3. (Colour online) Temperature dependence of uncorrelated MSD (empty circles) and the correlated MSRD_{\parallel} (full circles) for Co–O bond in LaCoO_3 and MSD (empty squares) and MSRD_{\parallel} (full red squares) for Co–O bond in $\text{La}_{0.5}\text{Sr}_{0.5}\text{Co}_{0.75}\text{Nb}_{0.25}\text{O}_3$. DCF is a displacement correlation function (difference between MSD and MSRD_{\parallel}).

dependence is less pronounced. The essentially large Co–O distance (Figure 2) and MSD (Figure 3) measured in this sample (Figure 2) presumably leading to a thicker surface HS and IS layers compared with the ones in LaCoO_3 sample. The fact that no increase of MSRD_{\parallel} was found in the temperature range from 5 to 20 K for $\text{La}_{0.5}\text{Sr}_{0.5}\text{Co}_{0.75}\text{Nb}_{0.25}\text{O}_3$ can be associated with a high correlation and low-amplitude motion between Co^{3+} ions in either LS or HS with the oxygen.

IV. CONCLUSIONS

We have observed an anomalous increase of the MSD of the Co–O bond in LaCoO_3 and $\text{La}_{0.5}\text{Sr}_{0.5}\text{Co}_{0.75}\text{Nb}_{0.25}\text{O}_3$ samples in temperature range from 50 to 17 K. Such increase of the MSD can be explained by the contribution of HS Co^{3+} located in the surface layer of powder grains (~ 500 nm) stabilized by the influence of structural defects and disruptions of chemical bonds (Fornasini *et al.*, 2004) assuming basic configuration of the cobalt ions as LS one, i.e. mix of different spin states from maximal ion radius in HS up to minimal one in LS.

A combined analysis of EXAFS and diffraction results above ~ 100 K have revealed an anomalous temperature dependence of the Co–O bond lengths in LaCoO_3 , while such dependence is absent in $\text{La}_{0.5}\text{Sr}_{0.5}\text{Co}_{0.75}\text{Nb}_{0.25}\text{O}_3$. Moreover, the temperature dependence of DCF is more pronounced in LaCoO_3 as compared to $\text{La}_{0.5}\text{Sr}_{0.5}\text{Co}_{0.75}\text{Nb}_{0.25}\text{O}_3$, particularly in vicinity of room temperature. The effects observed in $\text{La}_{0.5}\text{Sr}_{0.5}\text{Co}_{0.75}\text{Nb}_{0.25}\text{O}_3$, can be associated with essentially large amount of HS cobalt ions being in surface layers of crystallites compared to initial LaCoO_3 at low temperatures. Major part of cobalt ions retain LS-state configuration. It is owing to a significantly larger Co–O bond length for $\text{La}_{0.5}\text{Sr}_{0.5}\text{Co}_{0.75}\text{Nb}_{0.25}\text{O}_3$ sample.

Our experimental results are well described by a thermally induced spin-state transition of cobalt ions located in the surface layer of LaCoO_3 and $\text{La}_{0.5}\text{Sr}_{0.5}\text{Co}_{0.75}\text{Nb}_{0.25}\text{O}_3$ powders from HS to a highly hybridized IS spin state (Potze *et al.*, 1995).

The main conclusions of our work are in good agreement with existing data about magnetic susceptibility, magnetic circular dichroism and inelastic neutron scattering measurements, as well as with structural properties measured under high pressure (Potze *et al.*, 1995; Korotin *et al.*, 1996; Fornasini *et al.*, 2004; Knížek *et al.*, 2005; Haverkort *et al.*, 2006; Podlesnyak *et al.*, 2006; Pandey *et al.*, 2008; Herklotz *et al.*, 2009; Sundaram *et al.*, 2009; Troyanchuk *et al.*, 2013a, 2013b).

ACKNOWLEDGEMENTS

This work was supported by Russian Science Foundation project no. 15-19-20038.

- Fornasini, P., Beccara, G., Dalba, R., Grisenti, A., Sanson, M., and Vaccari, M. (2004). “Local dynamics, anharmonicity, and thermal expansion extended x-ray-absorption fine-structure measurements of copper,” *Phys. Rev. B* **70**, 174301.
- Haverkort, M. V., Hu, Z., Cezar, J. C., Burnus, T., Hartmann, H., Reuther, M., Zobel, C., Lorenz, T., Tanaka, A., Brookes, N. B., Hsieh, H. H., Lin, H. J., Chen, C. T., and Tjeng, L. H. (2006). “Spin state transition in LaCoO_3

- studied using soft X-ray absorption spectroscopy and magnetic circular dichroism," *Phys. Rev. Lett.* **97**, 176405.
- Herklotz, A., Rata, A. D., Schultz, L., and Doerr, K. (2009). "Reversible strain effect on the magnetization of LaCoO_3 films," *Phys. Rev. B* **79**, 092409.
- Knížek, K., Jirak, Z., Hejtmanek, J., Veverka, M., Marysko, M., and Maris, G. (2005). "Structural anomalies associated with the electronic and spin transitions in LnCoO_3 ," *Eur. Phys. J. B* **47**, 213.
- Korotin, M. A., Anisimov, V. I., Khomskii, D. I., Ezhov, S. Y., Solov'yev, I. V., Khomskii, D. I., and Sawatzky, G. A. (1996). "Intermediate-spin state and properties of LaCoO_3 ," *Phys. Rev. B* **54**, 5309.
- Kuzmin, A. (1995). "EDA: EXAFS data analysis software package," *Physica B* **208/209**, 175.
- Maris, G., Ren, Y., Volotchaev, V., Zobel, C., Lorenz, T., and Palstra, T. (2003). "Evidence for orbital ordering in LaCoO_3 ," *Phys. Rev. B* **67**, 224423.
- Pandey, S., Kumar, A., and Prabhakaran, D. (2008). "Investigation of the spin state of Co in LaCoO_3 at room temperature: *ab initio* calculations and high-resolution photoemission spectroscopy of single crystals," *Phys. Rev. B* **77**, 045123.
- Pirogov, A. N., Teplykh, E. A., Voronin, V. I., Balagurov, A. M., Pomjakushin, V. Y., Sikolenko, V. V., and Filonova, E. A. (1999). "Ferro- and antiferromagnetic ordering in LaMnO_3^{3+} ," *Phys. of the Sol. State* **41**, 91.
- Podlesnyak, A., Streule, S., Mesot, J., Medarde, M., Pomjakushina, E., Conder, K., Tanaka, A., Haverkort, M. V., and Khomskii, D. I. (2006). "Spin-state transition in LaCoO_3 : direct neutron spectroscopic evidence of excited magnetic states," *Phys. Rev. Lett.* **97**, 247208.
- Potze, R. H., Sawatzky, G. A., and Abbate, M. (1995). "Possibility for an intermediate-spin ground state in the charge-transfer material SrCoO_3 ," *Phys. Rev. B* **51**, 11501.
- Radaelli, P. G. and Cheong, S. W. (2002). "Structural phenomena associated with the spin-state transition in LaCoO_3 ," *Phys. Rev. B* **66**, 094408.
- Rodriguez-Carvajal, J. (1993). "Recent advances in magnetic structure determination by neutron powder diffraction," *Physica B* **192**, 55.
- Sazonov, A. P., Troyanchuk, I. O., Gamari-Seale, H., Sikolenko, V. V., Stefanopoulos, K. L., Nicolaides, G. K., and Atanassova, Y. K. (2009). "Neutron diffraction study and magnetic properties of $\text{La}_{1-x}\text{Ba}_x\text{CoO}_3$ ($x = 0.2$ and 0.3)," *J. Phys.: Condens. Mater* **21**, 156004.
- Senaris-Rodriguez, M. A. and Goodenough, J. B. (1995). "Magnetic and transport properties of the system $\text{La}_{1-x}\text{Sr}_x\text{CoO}_{3-\delta}$ ($0 < x \leq 0.50$)," *J. Solid State Chem.* **118**, 323.
- Shannon, R. D. (1976). "Revised effective ionic radii and systematic studies of interatomic distances in halides and chalcogenides," *Acta Crystallogr. Sect. A* **32**, 751.
- Sikolenko, V., Efimov, V., Efimova, E., Sazonov, A., Ritter, C., Kuzmin, A., and Troyanchuk, I. (2009). "Neutron diffraction studies of structural and magnetic properties of niobium doped cobaltites," *J. Phys.: Condens. Matter* **21**, 436002.
- Sundaram, N., Jiang, Z., Anderson, I. E., Belanger, D. P., Booth, C. H., Bridges, F., Mitchell, J. F., Proffen, T., and Zheng, H. (2009). "Local structure of $\text{La}_{1-x}\text{Sr}_x\text{CoO}_3$ determined from EXAFS and neutron pair distribution function studies," *Phys. Rev. Lett.* **102**, 026401.
- Troyanchuk, I., Balagurov, A., Sikolenko, V., Efimov, V., and Sheptyakov, D. (2013a). "Very large magnetoresistance and spin state transition in Ba-doped cobaltites," *J. Appl. Phys.* **113**, 053909.
- Troyanchuk, I., Bushinsky, M., Sikolenko, V., Efimov, V., Ritter, C., Hansen, T., and Többens, D. M. (2013b). "Pressure induced antiferromagnet-ferromagnet transition in $\text{La}_{0.5}\text{Ba}_{0.5}\text{CoO}_{2.8}$ cobaltite," *Eur. Phys. J. B* **86**, 435.
- Zobel, C., Kriener, M., Bruns, D., Baier, J., Grüninger, M., Lorenz, T., Reutler, P., and Revcolevschi, A. (2002). "EXAFS and X-ray diffraction study of LaCoO_3 across the spin-state transition," *Phys. Rev. B* **66**, R020402.